PHYSICAL REVIEW D VOLUME 23, NUMBER 1 1 JANUARY 1981

Strangeness −2 and −3 baryons in a quark model with chromodynamics

Kuang-Ta Chao
Rutherford High Energy Laboratory, Chilton, Didcot, Oxon OX11 0QX, England and Department of Physics, Peking University, Peking, China

Nathan Isgur
Department of Physics, University of Toronto, Toronto M5S 1A7, Canada

Gabriel Karl
Department of Physics, University of Guelph, Guelph N1G 2W1, Canada

(Received 11 June 1980)

We employ a quark model with ingredients suggested by quantum chromodynamics to study strangeness −2 and −3 resonances. Predictions of the spectrum and decay couplings of such states are made based on previous studies of the nonstrange and strangeness −1 sectors.

I. INTRODUCTION

The application of various ideas suggested by quantum chromodynamics (QCD) to the study of the low-energy properties of hadrons—their spectrum, decays, moments, and so on—has proved to be quite fruitful. The QCD-like models which have been used in this regime are based on a two-component picture[1] in which the structure of hadrons is dominated by (1) a flavor-independent confinement introduced by hand in the form of potentials, bags, strings, etc., and (2) short-range forces of the type expected from one-gluon exchange. The first of these ideas is based on the picture that (in the static approximation) the confining forces between, say, a quark and an antiquark depend only on their colors and not on their flavors, i.e., that it is the color that counts. The second ingredient is introduced by assuming that the phenomenological confinement potential can be introduced in such a way as to embrace most of the effects of higher-order gluon exchanges so that the remainder of the interquark force may be approximated by the (color-dependent) one-gluon-exchange terms analogous to the one-photon-exchange terms which dominate atomic spectroscopy. The color hyperfine interactions are actually the most important of these latter interactions and are responsible for such prominant features as the Δ-N and ρ-π splittings.

The applications of this "soft-QCD" program have been quite extensive and have had considerable phenomenological success.[2-15] It is our intention here to extend these calculations to the $S=-2$ and -3 baryons associated with the low-lying SU(6) supermultiplets $(56,0^+)$, $(70,1^-)$, $(56',0^+)$, $(70,0^+)$, $(56,2^+)$, $(70,2^+)$, and $(20,1^+)$ which have been studied already for $S=0$ and -1. While the present data on $S=-2$ and -3 baryons are sparse they are constantly improving; we may even hope that by demonstrating the relevance of such data to testing the ideas of soft QCD we may encourage further work along these lines. Of course, we also feel that it is worthwhile to display the predictions of our model for these sectors *before* the data are in.

There are indeed several ways in which the Ξ's and Ω's will provide tests of soft-QCD models. If the confinement is flavor independent then, as shown in Ref. 3, SU(3) symmetry is "maximally" violated in excited baryons by the solutions of the confinement problem, as the baryons arrange themselves in ideally mixed configurations analogous to the ideally mixed states which occur in mesons. In such circumstances the use of the totally antisymmetrized SU(6) basis states becomes ill advised and (taking the case $S=-1$) another basis—the "*uds* basis" in which the strange quark is singled out as quark 3 but in which the nonstrange quarks are still antisymmetrized—is more appropriate. The *uds* basis states then diagonalize the confinement problem with eigenfunctions that correspond to separate excitations of the nonstrange and strange quarks. This leads to several dramatic effects. In the low-lying negative-parity baryons, for example, one has

$$\Lambda\tfrac{5}{2}^- = \frac{1}{\sqrt{2}}(ud-du)s\chi^s_{3/2}\psi^\rho_{11}\,, \tag{1}$$

$$\Sigma\tfrac{5}{2}^- = \frac{1}{\sqrt{2}}(ud+du)s\chi^s_{3/2}\psi^\lambda_{11}\,, \tag{2}$$

where $\chi^s_{3/2}$ is the $s=s_z=\frac{3}{2}$ spin wave function and ψ^ρ_{11} (ψ^λ_{11}) is the spatial wave function with $l=l_z=1$ in the relative coordinate of the nonstrange quarks (in the relative coordinate of the strange quark and the center of mass of the nonstrange quarks). Since the strange quark is heavier, ψ^λ has a lower frequency than ψ^ρ and $\Lambda\frac{5}{2}^-$ is heavier than $\Sigma\frac{5}{2}^-$ in reversal of the situation in the ground states. In the $J^P=\frac{1}{2}^-$ sector the lowest-lying Λ in the confinement potential is predicted to be

$$\Lambda\tfrac{1}{2}^- = \frac{1}{\sqrt{2}}(ud-du)s\chi^\rho\psi^\lambda, \tag{3}$$

where χ^ρ is an $s=\frac{1}{2}$ spin wave function antisymmetric in quarks 1 and 2; such a state, in SU(6) language, is a 50-50 mixture of $\Lambda_1{}^2(70,1^-)\frac{1}{2}^-$ and $\Lambda_8{}^2(70,1^-)\frac{1}{2}^-$.[4] Indeed, decay analyses[16] of $\Lambda(1405)\frac{1}{2}^-$ indicate that it is almost purely composed of the state (3); most of the small discrepancy, in addition, is explained by hyperfine mixing of ρ and λ-type oscillations. Since ρ-type states decouple from $\bar{K}N$ scattering,[3,4] the segregation of ρ and λ oscillations in this way leads to a pattern of decouplings of $S=-1$ resonances from $\bar{K}N$ phase-shift analyses which seem to be borne out experimentally. In the $S=-2$ resonances the introduction of the analogous "ssu basis" will lead to the prediction of similar effects with, in this case, a pattern of decouplings from $\Xi\pi$.

Another significant tenet of soft-QCD models is that the chromomagnetic moments of quarks, which control the strengths of the color hyperfine interactions, are inversely proportional to the quark masses. Thus, for example, one has roughly

$$\frac{K^*-K}{\rho-\pi} \simeq \frac{m_d}{m_s} \tag{4}$$

and

$$\frac{\Sigma-\Lambda}{\Delta-N} \simeq \frac{2}{3}\left(1-\frac{m_d}{m_s}\right). \tag{5}$$

In baryons with two or three strange quarks these types of effects should become even stronger providing a clear test of the simple one-gluon-exchange form of the color hyperfine interactions.

In the next section we present the model and its solutions, all in terms of parameters previously established in the $S=0$ and -1 sectors.[7] In Sec. III we discuss our results and draw various preliminary conclusions.

II. THE HAMILTONIAN AND ITS SOLUTIONS

In the model we employ here[2-14] the Hamiltonian is

$$H=\sum_i m_i + H_0 + H_{\rm hyp}, \tag{6}$$

where

$$H_0 = \sum_i \frac{p_i^2}{2m_i} + \sum_{i<j} V^{ij}_{\rm conf} \tag{7}$$

and

$$H_{\rm hyp} = \sum_{i<j} \frac{2\alpha_s}{3m_i m_j}\left[\frac{8\pi}{3}\vec{S}_i\cdot\vec{S}_j\delta^3(\vec{r}_{ij}) + \frac{1}{r_{ij}^3}\left(\frac{3\vec{S}_i\cdot\vec{r}_{ij}\vec{S}_j\cdot\vec{r}_{ij}}{r_{ij}^2} - \vec{S}_i\cdot\vec{S}_j\right)\right], \tag{8}$$

and where $V^{ij}_{\rm conf}$ is the spin-independent potential into which is placed not only the empirical confinement potential but also the spin-independent parts of one-gluon exchange like $-\frac{2}{3}\alpha_s/r_{ij}$. As usual, chromomagnetic spin-orbit terms are dropped at this stage, it being presumed that they are strongly canceled by Thomas precession terms[4]; a discussion of the uncertainties in this procedure are reserved until later.

We now write

$$V^{ij}_{\rm conf} = \tfrac{1}{2}kr_{ij}^2 + U(r_{ij}) \tag{9}$$

and find approximate solutions by doing perturbation theory in U and $H_{\rm hyp}$. If we introduce the analog of the uds basis appropriate to the $S=-2$ sector by taking quarks 1 and 2 to be strange and quark 3 to be nonstrange, we are led to the flavor wave functions of the ssu basis,

$$\phi_{\Xi^0} = ssu, \tag{10}$$

$$\phi_{\Xi^-} = ssd, \tag{11}$$

and the relative coordinates

$$\vec{\rho} = \frac{1}{\sqrt{2}}(\vec{r}_1 - \vec{r}_2), \tag{12}$$

$$\vec{\lambda} = \frac{1}{\sqrt{6}}(\vec{r}_1 + \vec{r}_2 - 2\vec{r}_3), \tag{13}$$

in terms of which in the $U=H_{\rm hyp}=0$ limit we have

$$H_0 \to \tilde{H}_0 = \frac{p_\rho^2}{2m_\rho} + \frac{p_\lambda^2}{2m_\lambda} + \tfrac{3}{2}k(\rho^2+\lambda^2) \tag{14}$$

with

$$m_\rho = m_s \tag{15}$$

and

$$m_\lambda = \frac{3m_d m_s}{2m_s + m_d} < m_s. \tag{16}$$

The solutions to this Hamiltonian are wave functions

$$\psi^{xy}_{lm} = \tilde{\psi}^{xy}_{lm}\psi_{00}, \tag{17}$$

where

$$\psi_{00} = \frac{\alpha_\rho^{3/2}\alpha_\lambda^{3/2}}{\pi^{3/2}}\exp[-\tfrac{1}{2}(\alpha_\rho^2\rho^2 + \alpha_\lambda^2\lambda^2)] \tag{18}$$

and

$$\tilde{\psi}_{00} = 1, \tag{19}$$

$$\tilde{\psi}^\rho_{11} = \alpha_\rho\rho_+, \tag{20}$$

$$\tilde{\psi}^\lambda_{11} = \alpha_\lambda\lambda_+, \tag{21}$$

$$\tilde{\psi}_{00}^{\rho\rho} = (\tfrac{2}{3})^{1/2}\alpha_\rho^2(\rho^2 - \tfrac{3}{2}\alpha_\rho^{-2}) , \tag{22}$$

$$\tilde{\psi}_{00}^{\rho\lambda} = \frac{2}{\sqrt{3}}\alpha_\rho\alpha_\lambda\vec{\rho}\cdot\vec{\lambda} , \tag{23}$$

$$\tilde{\psi}_{00}^{\lambda\lambda} = (\tfrac{2}{3})^{1/2}\alpha_\lambda^2(\lambda^2 - \tfrac{3}{2}\alpha_\lambda^{2}) , \tag{24}$$

$$\tilde{\psi}_{11}^{\rho\lambda} = \alpha_\rho\alpha_\lambda(\rho_+\lambda_z - \rho_z\lambda_+) , \tag{25}$$

$$\tilde{\psi}_{22}^{\rho\rho} = (\tfrac{1}{2})^{1/2}\alpha_\rho^2\rho_+^2 , \tag{26}$$

$$\tilde{\psi}_{22}^{\rho\lambda} = \alpha_\rho\alpha_\lambda\rho_+\lambda_+ , \tag{27}$$

$$\tilde{\psi}_{22}^{\lambda\lambda} = (\tfrac{1}{2})^{1/2}\alpha_\lambda^2\lambda_+^2 , \tag{28}$$

where

$$\alpha_i = (3km_i)^{1/4} , \tag{29}$$

which have energies $(n_\rho + \frac{3}{2})\omega_\rho + (n_\lambda + \frac{3}{2})\omega_\lambda$, where

$$\omega_i = \left(\frac{3k}{m_i}\right)^{1/2} , \tag{30}$$

and where n_i is the number of units of excitation of the $i = \rho, \lambda$ variable. Thus, for example

$$E[\psi^\lambda] - E[\psi^\rho] = \omega_\lambda - \omega_\rho > 0 , \tag{31}$$

since $m_\rho > m_\lambda$; this is the analog of the $\Lambda\frac{5}{2}^- > \Sigma\frac{5}{2}^-$ effect in $S = -1$ baryons mentioned in the Introduction.

When U differs from zero it can be shown[5,11] that (in first-order perturbation theory) its effects may be described very simply: In the SU(3) limit one has in terms of three constants E_0, Ω, and Δ determined in the $S = 0$ sector

$$E[\psi_{00}] = E_0 , \tag{32}$$

$$E[\psi_{1m}^\rho] = E[\psi_{1m}^\lambda] = E_0 + \Omega , \tag{33}$$

$$E[\psi_{00}^{\rho\rho}] = E[\psi_{00}^{\lambda\lambda}] = E_0 + 2\Omega - \tfrac{3}{4}\Delta , \tag{34}$$

$$\langle\psi_{00}^{\rho\rho}|H_0|\psi_{00}^{\lambda\lambda}\rangle = -\tfrac{1}{4}\Delta , \tag{35}$$

$$E[\psi_{00}^{\rho\lambda}] = E_0 + 2\Omega - \tfrac{1}{2}\Delta , \tag{36}$$

$$E[\psi_{11}^{\rho\lambda}] = E_0 + 2\Omega , \tag{37}$$

$$E[\psi_{2m}^{\rho\rho}] = E[\psi_{2m}^{\lambda\lambda}] = E_0 + 2\Omega - \tfrac{3}{10}\Delta , \tag{38}$$

$$\langle\psi_{2m}^{\rho\rho}|H_0|\psi_{2m}^{\lambda\lambda}\rangle = -\tfrac{1}{10}\Delta , \tag{39}$$

$$E[\psi_{2m}^{\rho\lambda}] = E_0 + 2\Omega - \tfrac{1}{5}\Delta . \tag{40}$$

To break SU(3) we take the prescription that ρ and λ excitation energies are decreased by $(m_d/m_\rho)^{1/2}$ and $(m_d/m_\lambda)^{1/2}$, respectively, as they would be in the harmonic limit. We then find the confinement energies shown in Table I. [Columns 3 and 4 of the table follow from extrapolation by this method of columns 1 and 2, which consist of the actual numbers used in Refs. 4, 5, and 7; the table is therefore not actually based on the formulas (32)–(40) which were found later,[11] but in no case is the deviation from them very significant. We have in addition assumed for completeness that the $\rho\rho \leftrightarrow \lambda\lambda$ mixing terms have the same dependence as the $\rho\lambda \leftrightarrow \rho\lambda$ terms, but this assumption has practically no influence on our results.]

The complete Hamiltonian of the model may be obtained by calculating the hyperfine matrix elements which may be obtained from those of Refs. 4, 5, and 7 for the $S = 0$ and -1 sectors by making the interchange $m_u \leftrightarrow m_s$ everywhere. The problem may then be diagonalized sector by sector to obtain the spectrum and composition of $S = -2$ and -3 baryons. [The results for the ground and negative-parity states have been given in Refs. 7 and 4, respectively, but we quote the (slightly updated[7]) results here both for completeness and to make them available in the "standard" conventions of Ref. 10.] Finally, we use these predictions in conjunction with a recent decay model[9,10] to calculate the decay widths of these resonances. Since the parameters of the emission model are known, we can be completely predictive. Our results are summarized in Tables II and III which give the spectrum, approximate compositions, and decay amplitudes (whose squares are the partial widths to the indicated channels) of all of the resonances. Figures 1 and 2 display our results graphically.

III. DISCUSSION AND CONCLUSION

In the absence of much data on these states, we feel that a detailed sector-by-sector analysis of these results is premature; we concentrate our remarks instead on some general features.

First, with respect to spectroscopy: As with other work on this model, the splittings within a given harmonic-oscillator-associated band are believed to be more reliable than the overall posi-

TABLE I. The confinement energies in MeV.

	Confinement energy in $S=0$	in $S=-1$	in $S=-2$	in $S=-3$
$E[\psi_{00}^0]$	1135	1295	1455	1615
$E[\psi_{1m}^\rho]$	1610	1770	1825	1985
$E[\psi_{1m}^\lambda]$	1610	1700	1895	1985
$E[\psi_{00}^{\rho\rho}]$	1705	1895	1910	2070
$E[\psi_{00}^{\rho\lambda}]$	1810	1945	2040	2150
$E[\psi_{00}^{\lambda\lambda}]$	1705	1805	2000	2070
$\langle\psi_{00}^{\rho\rho}\|H_0\|\psi_{00}^{\lambda\lambda}\rangle$	−105	−100	−90	−85
$E[\psi_{1m}^{\rho\lambda}]$	2020	2145	2225	2315
$E[\psi_{2m}^{\rho\rho}]$	1890	2085	2055	2215
$E[\psi_{2m}^{\rho\lambda}]$	1935	2065	2150	2245
$E[\psi_{2m}^{\lambda\lambda}]$	1890	1975	2175	2215
$\langle\psi_{2m}^{\rho\rho}\|H_0\|\psi_{2m}^{\lambda\lambda}\rangle$	−40	−40	−35	−35

TABLE II. Calculated spectrum and composition in the $S=-2$ sector in the ssu and in the SU(6) bases and the resulting decay amplitudes.

State (J^P)	Mass (MeV)	Approximate composition in the ssu basis	Approximate composition in the SU(6) basis	Decay amplitudes (MeV$^{1/2}$) $\Xi\pi$	$\Sigma\bar{K}$	$\Lambda\bar{K}$	$\Xi^*\pi$	
							P wave	
$\Xi\frac{1}{2}^+$	1325	$+0.95\,{}^2S+\cdots$	$+0.95\Xi_8\,{}^2S_S+\cdots$	$\cdots$	$\cdots$	$\cdots$	$\cdots$	
	1695	$+0.73\,{}^2S_{\rho\rho}+0.67\,{}^2S_{\lambda\lambda}+\cdots$	$+0.99\Xi_8\,{}^2S'_S+\cdots$	−1.0	+0.2	+0.7	−0.2	
	1950	$+0.51\,{}^2S_{\rho\rho}-0.62\,{}^2S_{\rho\lambda}-0.51\,{}^2S_{\lambda\lambda}+\cdots$	$+0.95\Xi_8\,{}^2S_M+\cdots$	−1.8	−3.4	−2.6	−2.3	
	2065	$+0.93\,{}^4D_{\rho\rho}+\cdots$	$+0.72\Xi_{10}\,{}^4D_S+0.59\Xi_8\,{}^4D_M+\cdots$	−0.5	−4.1	+2.1	0.0	
	2105	$-0.43\,{}^2S_{\rho\rho}-0.65\,{}^2S_{\rho\lambda}+0.53\,{}^2S_{\lambda\lambda}+\cdots$	$+0.94\Xi_{10}\,{}^2S_M+\cdots$	+0.1	+0.8	−1.4	+4.0	
	2155	$+0.85\,{}^4D_{\lambda\lambda}-0.41\,{}^2P_{\rho\lambda}+\cdots$	$+0.67\Xi_{10}\,{}^4D_S-0.53\Xi_8\,{}^4D_M-0.41\Xi_8\,{}^2P_A+\cdots$	−4.0	−0.6	+2.0	+0.6	
	2255	$+0.43\,{}^4D_{\lambda\lambda}+0.88\,{}^2P_{\rho\lambda}+\cdots$	$-0.45\Xi_8\,{}^4D_M+0.88\Xi_8\,{}^2P_A+\cdots$	−1.9	+0.6	0.0	+0.8	
							P wave	F wave
$\Xi\frac{3}{2}^+$	1530	$+0.97\,{}^4S+\cdots$	$+0.97\Xi_{10}\,{}^2S_S+\cdots$	+4.5	$\cdots$	$\cdots$	$\cdots$	$\cdots$
	1930	$+0.90\,{}^2D_{\rho\rho}+\cdots$	$+0.80\Xi_8\,{}^2D_S-0.54\Xi_8\,{}^2D_M+\cdots$	−0.1	+4.3	+2.1	+0.3	−0.4
	1965	$+0.88\,{}^4S_{\rho\rho}+0.42\,{}^4S_{\lambda\lambda}+\cdots$	$+0.92\Xi_{10}\,{}^4S'_S+0.32\Xi_8\,{}^2S_M+\cdots$	+1.6	+4.1	−3.0	+2.0	−0.2
	2070	$+0.47\,{}^4S_{\lambda\lambda}+0.79\,{}^4D_{\rho\rho}+\cdots$	$+0.49\Xi_8\,{}^4S_M-0.58\Xi_{10}\,{}^4D_S-0.54\Xi_8\,{}^4D_M+\cdots$	−2.4	+2.7	−2.2	−2.2	−0.5
	2125	$+0.72\,{}^4S_{\lambda\lambda}-0.54\,{}^4D_{\rho\rho}+\cdots$	$-0.31\Xi_{10}\,{}^4S'_S+0.71\Xi_8\,{}^4S_M+0.58\Xi_{10}\,{}^4D_S+\cdots$	−4.6	−0.8	+1.2	−2.9	0.0
	2175	$+0.82\,{}^2D_{\rho\lambda}+\cdots$	$+0.31\Xi_8\,{}^4D_M+0.86\Xi_{10}\,{}^2D_M+\cdots$	+1.9	0.0	−1.1	−0.6	+0.6
	2185	$+0.43\,{}^2D_{\rho\lambda}+0.33\,{}^2D_{\lambda\lambda}+0.65\,{}^4D_{\lambda\lambda}$ $+0.42\,{}^2P_{\rho\lambda}+\cdots$	$+0.32\Xi_8\,{}^4S_M-0.46\Xi_{10}\,{}^4D_S-0.46\Xi_8\,{}^2D_M$ $+0.46\Xi_8\,{}^4D_M-0.42\Xi_8\,{}^2P_A+\cdots$	+1.3	+0.9	−0.3	−3.1	+0.1
	2215	$+0.82\,{}^2D_{\lambda\lambda}-0.46\,{}^2P_{\rho\lambda}+\cdots$	$-0.44\Xi_8\,{}^2D_S-0.59\Xi_8\,{}^2D_M+0.43\Xi_{10}\,{}^2D_M$ $+0.46\Xi_8\,{}^2P_A+\cdots$	+0.9	−0.3	+0.2	−0.9	+5.6
	2255	$-0.59\,{}^4D_{\lambda\lambda}+0.73\,{}^2P_{\rho\lambda}+\cdots$	$+0.58\Xi_8\,{}^4D_M+0.73\Xi_8\,{}^2P_A+\cdots$	+1.2	+0.1	−0.1	−1.7	−4.1
							P wave	F wave
$\Xi\frac{5}{2}^+$	1935	$+0.93\,{}^2D_{\rho\rho}+\cdots$	$+0.83\Xi_8\,{}^2D_S-0.54\Xi_8\,{}^2D_M+\cdots$	−0.5	+4.9	+1.9	+0.6	−0.3
	2110	$+0.95\,{}^4D_{\rho\rho}+\cdots$	$+0.85\Xi_{10}\,{}^4D_S+0.50\Xi_8\,{}^4D_M+\cdots$	+0.8	+2.5	−3.0	+0.8	+0.8
	2170	$+0.94\,{}^2D_{\rho\lambda}+\cdots$	$+0.51\Xi_8\,{}^2D_M+0.82\Xi_{10}\,{}^2D_M+\cdots$	−0.2	−0.2	−2.4	−0.3	−0.2
	2200	$-0.92\,{}^2D_{\lambda\lambda}+\cdots$	$-0.49\Xi_8\,{}^2D_S-0.63\Xi_8\,{}^2D_M+0.52\Xi_8\,{}^4D_M+\cdots$	+4.9	−0.6	0.0	−2.1	+5.3
	2240	$-0.92\,{}^4D_{\lambda\lambda}+\cdots$	$-0.47\Xi_{10}\,{}^4D_S+0.83\Xi_{10}\,{}^2D_M+\cdots$	−2.9	−0.4	+0.5	−3.7	−3.3
								F wave
$\Xi\frac{7}{2}^+$	2085	$+0.99\,{}^4D_{\rho\rho}+\cdots$	$+0.81\Xi_{10}\,{}^4D_S+0.59\Xi_8\,{}^4D_M$	+1.0	+4.2	−5.4		+0.5
	2195	$+0.99\,{}^4D_{\lambda\lambda}+\cdots$	$+0.59\Xi_{10}\,{}^4D_S-0.81\Xi_8\,{}^4D_M$	+8.6	+1.0	−1.1		+4.6

TABLE II. (*Continued*)

State (J^P)	Mass (MeV)	Approximate composition in the *ssu*	Approximate composition in the SU(6) basis	Decay amplitudes (MeV$^{1/2}$) $\Xi\pi$	$\Sigma\bar{K}$	$\Lambda\bar{K}$	$\Xi^*\pi$ *S* wave	$\Xi^*\pi$ *D* wave
$\Xi\frac{1}{2}^-$	1785	$+0.39\,{}^4P_\lambda-0.46\,{}^2P_\lambda+0.80\,{}^2P_\rho$	$-0.39\Xi_8\,{}^4P_M+0.89\Xi_8\,{}^2P_M+0.24\Xi_{10}\,{}^2P_M$	−3.6	−3.7	−4.2	+0.6	
	1890	$+0.75\,{}^4P_\lambda+0.34\,{}^2P_\lambda+0.56\,{}^2P_\rho$	$+0.75\Xi_8\,{}^4P_M+0.16\Xi_8\,{}^2P_M+0.64\Xi_{10}\,{}^2P_M$	+5.5	−2.2	+0.8	−0.4	
	1925	$+0.53\,{}^4P_\lambda+0.82\,{}^2P_\lambda+0.21\,{}^2P_\rho$	$-0.53\Xi_8\,{}^4P_M-0.43\Xi_8\,{}^2P_M+0.73\Xi_{10}\,{}^2P_M$	−1.5	+5.4	−1.4	−6.7	
$\Xi\frac{3}{2}^-$	1800	$-0.08\,{}^4P_\lambda-0.45\,{}^2P_\lambda+0.89\,{}^2P_\rho$	$+0.08\Xi_8\,{}^4P_M+0.95\Xi_8\,{}^2P_M+0.31\Xi_{10}\,{}^2P_M$	+1.6	+3.9	+3.6	+1.6	+0.8
	1910	$+0.10\,{}^4P_\lambda+0.88\,{}^2P_\lambda+0.46\,{}^2P_\rho$	$-0.10\Xi_8\,{}^4P_M-0.30\Xi_8\,{}^2P_M+0.95\Xi_{10}\,{}^2P_M$	−4.3	−4.6	+0.9	−3.7	−3.9
	1970	$+0.99\,{}^4P_\lambda-0.12\,{}^2P_\lambda+0.02\,{}^2P_\rho$	$+0.99\Xi_8\,{}^4P_M-0.10\Xi_8\,{}^2P_M+0.07\Xi_{10}\,{}^2P_M$	+3.7	−3.2	+1.8	−5.2	+4.3
$\Xi\frac{5}{2}^-$	1920	${}^4P_\lambda$	$\Xi_8\,{}^4P_M$	+9.8	−3.4	+4.7		+4.2

tions of the bands. If, for example, the positive-parity excited Ξ's were to lie consistently 20 MeV above our predictions we would not be much surprised or dismayed; on the other hand, confirmation of a pattern of states like that displayed in the figures would constitute evidence in favor of the soft-QCD quark dynamics we have employed. If the model fails, we would anticipate that its most vulnerable feature, the semiempirical treatment of spin-orbit forces, would be involved.

Turning next to the predicted compositions of these states (and the resultant decay amplitudes), we note from Table II that apart from the states involving S_S and S_M (where the U mixing of ρ- and λ-type modes is very strong), the nonsymmetrized *ssu* basis usually provides a much simplified picture of the states. Thus, for example, the five $\Xi\frac{5}{2}^+$ states are all nearly pure in this basis and one can immediately predict that the lowest three will decouple from $\Xi\pi$ and $\Xi^*\pi$; in the SU(6) basis the same states appear to be very complicated. Another particularly striking test which may be very amenable to study occurs in the $\Xi\frac{7}{2}^+$ sector where ρ-λ segregation predicts states at 2085 and 2195 MeV; the lower almost decouples from $\Xi\pi$ and $\Xi^*\pi$ but should be strong in $\Sigma\bar{K}$ and $\Lambda\bar{K}$ while the upper resonance has the opposite pattern of couplings. Of course, the simplicity of the *ssu* basis description is sometimes masked by hyperfine mixing; this is the case in the $\Xi\frac{1}{2}^-$ and $\Xi\frac{3}{2}^-$ sectors, where ${}^2\rho$-${}^2\lambda$ mixing is reasonably strong, but even in these cases the probability of ${}^2\rho$ in the lowest-lying states remains much larger than ${}^2\lambda$ (the Ξ's are somewhat more pure than the Σ's because the hyperfine interactions have become weaker). In general, confirmation of this pattern of ρ-λ segregation with its concomitant decouplings would provide further quite strong evidence for the flavor independence of quark confinement.

ACKNOWLEDGMENTS

K.-T.C. would like to express his gratitude to Dick Roberts and the entire Theory Division of the Rutherford Laboratory for their help and hospitality during his visit. N. I. and G. K. acknowledge with appreciation the Department of Theoretical Physics of Oxford University and the Theory Division of Rutherford Laboratory, respectively, where they were on leave when this work was begun. This research was supported in part by the Natural Sciences and Engineering Research Council, Canada.

APPENDIX

In this appendix we make some of our conventions explicit to facilitate comparison with other work.

TABLE III. Calculated spectrum and composition in the $S=-3$ sector and the resulting decay amplitudes.

State (J^P)	Mass (MeV)	Approximate composition	Decay amplitude ($MeV^{1/2}$) $\Xi\bar{K}$	$\Xi^*\bar{K}$		$\Omega\eta$	
				P wave		*P* wave	
$\Omega\frac{1}{2}^+$	2190	$+0.74\,^2S_M+0.67\,^4D_S$	+2.2	−4.4		....	
	2210	$+0.67\,^2S_M-0.74\,^4D_S$	+6.1	+2.3		....	
				P wave	*F* wave	*P* wave	*F* wave
$\Omega\frac{3}{2}^+$	1675	$+0.98\,^4S_S+\cdots$	....	....	....	....	....
	2065	$+0.99\,^4S'_S+\cdots$	+5.4	+2.2	+0.1	....	....
	2215	$+0.98\,^4D_S+\cdots$	−5.0	+2.6	+1.2	....	....
	2265	$+0.98\,^2D_M+\cdots$	+0.9	−0.4	+4.0	−0.2	−0.5
				P wave	*F* wave	*P* wave	*F* wave
$\Omega\frac{5}{2}^+$	2225	$+0.99\,^4D_S+\cdots$	+10.0	+3.1	+2.6	0.0	0.0
	2265	$+0.99\,^2D_M+\cdots$	−1.6	+3.3	−2.0	−1.3	−0.3
				F wave		*F* wave	
$\Omega\frac{7}{2}^+$	2210	^4D_S	+8.0	+2.4		....	
				S wave		*S* wave	
$\Omega\frac{1}{2}^-$	2020	^2P_M	+3.1	....		....	
				S wave	*D* wave	*S* wave	*D* wave
$\Omega\frac{3}{2}^-$	2020	^2P_M	−3.9	....	....	....	....

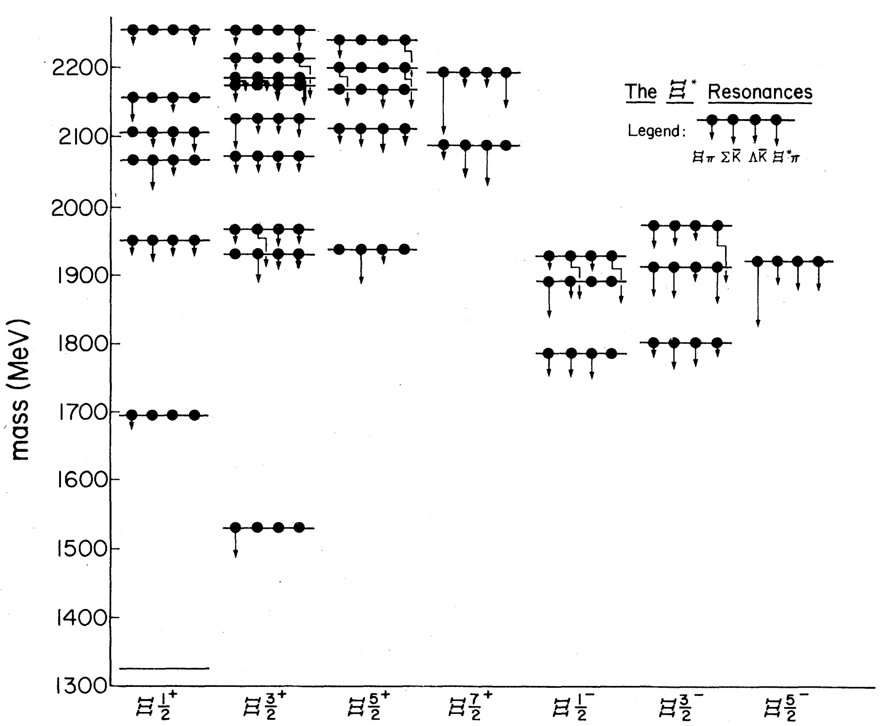

FIG. 1. The predicted spectrum of $S=-2$ resonances and their decay patterns. The length of an arrow is proportional to the *amplitude* for decay of the resonance to the channel indicated in the legend (i.e., to $\Xi\pi$, $\Sigma\bar{K}$, $\Lambda\bar{K}$, or $\Xi^*\pi$).

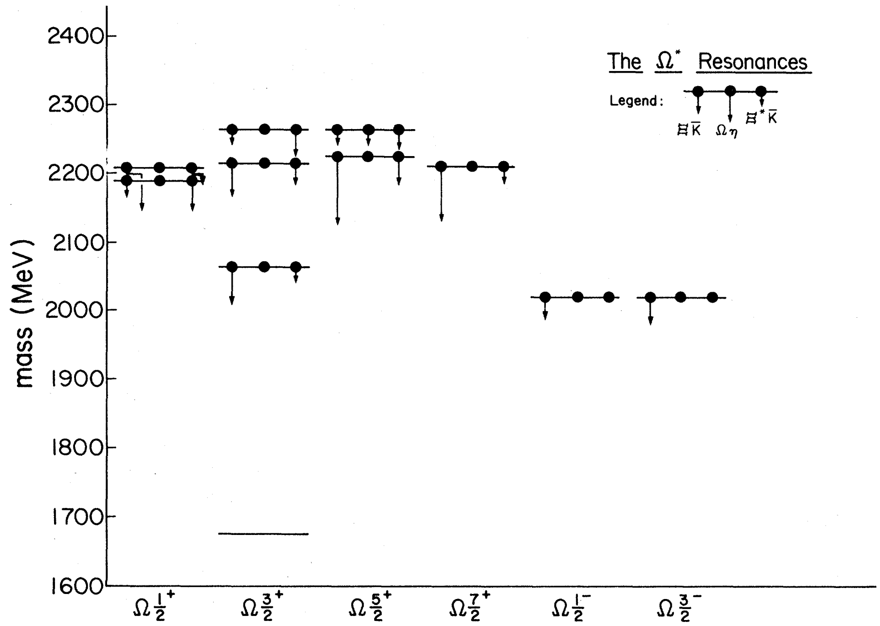

FIG. 2. As in Fig. 1, but for $S=-3$ resonances.

We use here the "standard" conventions of Ref. 10 in which the Ξ-flavor wave functions are

$$\phi^{\rho}_{\Xi^0}=\frac{1}{\sqrt{2}}(sus-uss)\,, \tag{A1}$$

$$\phi^{\lambda}_{\Xi^0}=-\frac{1}{\sqrt{6}}(sus+uss-2ssu)\,, \tag{A2}$$

and

$$\phi^{s}_{\Xi^0}=\frac{1}{\sqrt{3}}(ssu+sus+uss)\,. \tag{A3}$$

With these conventions the relation between the ssu basis of Eqs. (10) and (11) of the main body of the text and the SU(6) basis is that

$$\Xi_8\,{}^2S_s \leftrightarrow +\Xi\,{}^2S\,, \tag{A4}$$

$$\Xi_{10}\,{}^4S_s \leftrightarrow +\Xi\,{}^4S \tag{A5}$$

for the $N=0$ levels,

$$\Xi_8\,{}^2P_M \leftrightarrow -\frac{1}{\sqrt{2}}(\Xi\,{}^2P_\rho-\Xi\,{}^2P_\lambda)\,, \tag{A6}$$

$$\Xi_{10}\,{}^2P_M \leftrightarrow -\frac{1}{\sqrt{2}}(\Xi\,{}^2P_\rho+\Xi\,{}^2P_\lambda)\,, \tag{A7}$$

$$\Xi_8\,{}^4P_M \leftrightarrow +\Xi\,{}^4P_\lambda \tag{A8}$$

for the $N=1$ levels, while

$$\Xi_8\,{}^2L_s \leftrightarrow +\frac{1}{\sqrt{2}}(\Xi\,{}^2L_{\rho\rho}+\Xi\,{}^2L_{\lambda\lambda})\,, \tag{A9}$$

$$\Xi_{10}\,{}^4L_s \leftrightarrow +\frac{1}{\sqrt{2}}(\Xi\,{}^4L_{\rho\rho}+\Xi\,{}^4L_{\lambda\lambda})\,, \tag{A10}$$

$$\Xi_8\,{}^2L_M \leftrightarrow +\frac{1}{\sqrt{2}}\Xi\,{}^2L_{\rho\lambda}-\frac{1}{2}\Xi\,{}^2L_{\rho\rho}+\frac{1}{2}\Xi\,{}^2L_{\lambda\lambda}\,, \tag{A11}$$

$$\Xi_{10}\,{}^2L_M \leftrightarrow +\frac{1}{\sqrt{2}}\Xi\,{}^2L_{\rho\lambda}+\frac{1}{2}\Xi\,{}^2L_{\rho\rho}-\frac{1}{2}\Xi\,{}^2L_{\lambda\lambda}\,, \tag{A12}$$

$$\Xi_8\,{}^4L_M \leftrightarrow \frac{1}{\sqrt{2}}(\Xi\,{}^4L_{\rho\rho}-\Xi\,{}^4L_{\lambda\lambda})\,, \tag{A13}$$

$$\Xi_8\,{}^2P_A \leftrightarrow +\Xi\,{}^2P_{\rho\lambda}\,. \tag{A14}$$

---

[1] A. De Rújula, H. Georgi, and S. L. Glashow, Phys. Rev. D 12, 147 (1975); T. DeGrand, R. L. Jaffe, K. Johnson, and J. Kiskis, *ibid.* 12, 2060 (1975).

[2] Nathan Isgur and Gabriel Karl, Phys. Lett 72B, 109 (1977).

[3] Nathan Isgur and Gabriel Karl, Phys. Lett. 74B, 353 (1978).

[4] Nathan Isgur and Gabriel Karl, Phys. Rev. D 18, 4187 (1978).

[5] Nathan Isgur and Gabriel Karl, Phys. Rev. D 19, 2653 (1979); erratum *ibid.* (to be published).

[6] L. A. Copley, Nathan Isgur, and Gabriel Karl, Phys. Rev. D 20, 768 (1979).

[7] Nathan Isgur and Gabriel Karl, Phys. Rev. D 20, 1191 (1979). We use this paper's updated parameters here.

[8] Nathan Isgur, Gabriel Karl, and Roman Koniuk, Phys. Rev. Lett. 41, 1269 (1978).

[9] Roman Koniuk and Nathan Isgur, Phys. Rev. Lett. 44,

845 (1980).

[10]Roman Koniuk and Nathan Isgur, Phys. Rev. D 21, 1868 (1980).

[11]Nathan Isgur, in *Proceedings of the XVI International School of Subnuclear Physics, Erice, Italy, 1978,* edited by A. Zichichi (Plenum, New York, 1980).

[12]Gabriel Karl, in *Proceedings of the 19th International Conference on High Energy Physics, Tokyo, 1978,* edited by S. Homma, M. Kawaguchi, and H. Miyazawa (Phys. Soc. of Japan, Tokyo, 1979), p. 135.

[13]O. W. Greenberg, Annu. Rev. Nucl. Part. Sci. 28, 327 (1978).

[14]A. J. G. Hey, summary talk in Proceedings of the 1979 European Physical Society International Conference on High Energy Physics, Geneva (unpublished).

[15]For a listing of work on models of baryons and mesons related to Refs. 2 to 14, see Ref. 10.

[16]A. J. G. Hey, P. J. Litchfield, and R. J. Cashmore, Nucl. Phys. B95, 516 (1975); D. Faiman and D. E. Plane, *ibid.* B50, 379 (1972).